Transplant International

Transplant International ISSN 0934-0874

ORIGINAL ARTICLE

Rapamycin, but not cyclosporine A, inhibits vascularization and incorporation of implanted surgical meshes

Matthias W. Laschke,[1] Jörg M. Häufel,[1] Jonas Roller,[1] Heike Schorr[2] and Michael D. Menger[1]

1 Institute for Clinical & Experimental Surgery, University of Saarland, Homburg/Saar, Germany
2 Department of Clinical Chemistry and Central Laboratory Medicine, University Hospital of Saarland, Homburg/Saar, Germany

Keywords
angiogenesis, cyclosporine, hernia repair, immunosuppression, rapamycin, surgical mesh.

Correspondence
Dr med. Matthias W. Laschke, Institute for Clinical & Experimental Surgery, University of Saarland, D-66421 Homburg/Saar, Germany. Tel.: +49 6841 162 6554; fax: +49 6841 162 6553; e-mail: matthias.laschke@uniklinik-saarland.de

Received: 8 September 2008
Revision requested: 29 September 2008
Accepted: 8 January 2009

doi:10.1111/j.1432-2277.2009.00841.x

Summary

Incisional hernias are a frequent complication of upper abdominal wall interventions, especially in patients undergoing liver transplantation with subsequent immunosuppressive therapy. Therefore, we analyzed in this study the manner in which the incorporation of a surgical mesh for hernia repair is affected by the immunosuppressant drugs rapamycin and cyclosporine A (CsA). For this purpose, Ultrapro meshes were implanted into the dorsal skinfold chambers of rapamycin- and CsA-treated hamsters. Untreated animals served as controls. The angiogenic and inflammatory host tissue response to the mesh implants was then analyzed over a 14-day period by means of intravital fluorescence microscopy. Mesh incorporation was determined by histology and measurement of explantation strength. Rapamycin dose-dependently inhibited vascularization of implanted meshes, as indicated by a significantly reduced number of angiogenesis-positive regions of interest and microvessel density, when compared with CsA-treated hamsters and controls. In addition, the granulation tissue surrounding the meshes of rapamycin-treated animals exhibited only a low collagen content, resulting in an impaired mesh incorporation with a significantly reduced explantation strength. Leukocyte–endothelial cell interaction did not show marked differences between the observation groups. Thus, immunosuppressed patients should not be treated with rapamycin in case of incisional hernia repair in order to guarantee adequate mesh incorporation.

Introduction

Incisional hernias represent a common complication of upper and lower abdominal wall interventions, including transplantation of the pancreas, the kidney and the liver. In fact, the incidence of hernias following orthotopic liver transplantation even seems to have increased during the preceding years [1]. For instance, Toso *et al.* [2] recently reported that 34.3% (24 of 70) of their patients suffered from this complication. In general, there are several causal factors that can contribute to the formation of incisional hernias after liver transplantation. Increased mechanical strain on the wound may be induced as a result of the discrepancy between the size of the transplanted organ and too little space within the abdomen or resulting from substantial postoperative ascites in the abdominal cavity [3]. Moreover, liver transplant patients are treated by high-dose immunosuppressive drugs, which have been shown to significantly impair wound healing by inhibiting angiogenesis and collagen synthesis [4–6]. This applies in particular to rapamycin. Nonetheless, patients are treated with this immunosuppressant drug because of intolerance of tacrolimus or worsening renal function after transplantation [7].

During the last few years, implantation of surgical meshes has become the gold standard in the treatment of incisional hernias. In comparison to primary suture repair, this technique results in significantly reduced recurrence rates [8]. In principle, mesh implantation can be conducted either by open prosthetic repair or laparo-

scopically [9], and laparoscopic hernia repair is associated with fewer wound complications and a decreased incidence of recurrence [7]. However, in both cases adequate mesh incorporation into the surrounding tissue is a major prerequisite for the long-term stability of the closed abdominal wall defect and, thus, for the success of the method.

Based on the finding that immunosuppressive therapy impairs the formation of granulation tissue during wound healing, the aim of the present *in vivo* study was to analyze the manner in which the immunosuppressive drugs rapamycin and cyclosporine A (CsA) affect the incorporation of implanted surgical meshes. For this purpose, we implanted an Ultrapro mesh into the dorsal skinfold chamber of rapamycin- or CsA-treated hamsters, as described previously [10,11]. Subsequently, we analyzed angiogenesis, vascularization and activation of leukocytes at the implantation site as well as mesh incorporation by means of intravital fluorescence microscopy and histology.

Materials and methods

Animals

Eight- to ten-week-old male Syrian golden hamsters with a body weight of 60–80 g were used for the experiments. They were housed one per cage and had free access to tap water and standard pellet food (Altromin, Lage, Germany). The experiments were conducted in accordance with the German legislation on protection of animals and the NIH Guidelines for the Care and Use of Laboratory Animals (NIH Publication #85-23 Rev. 1985). They were approved by the local governmental animal care committee.

Preparation of the dorsal skinfold chamber

The hamster dorsal skinfold chamber and its implantation procedure have been described previously in detail [12,13]. In brief, under sodium pentobarbital anesthesia (50 mg/kg body weight i.p.), two symmetrical titanium frames were implanted on the extended dorsal skinfold of the hamsters, so that they sandwiched the double layer of skin. One layer of skin was completely removed in a circular area of approximately 15 mm in diameter, and the remaining layers (consisting of striated skin muscle, subcutaneous tissue and cutis) were covered with a removable coverslip incorporated into one of the titanium frames (Fig. 1a). After the preparation, the hamsters were allowed to recover from anesthesia and surgery for at least 48 h. The animals tolerated the chamber and its preparation well, as indicated by constant body weight as well as normal feeding and sleeping habits.

Mesh implantation

In this study, we implanted a small piece (approximately 3×3 mm) of an Ultrapro mesh (kindly provided by Ethicon Products, Norderstedt, Germany) into the dorsal skinfold chamber. This Prolene–Monocryl composite mesh is commonly used in clinical practice for hernia repair. For mesh implantation, the animals were anesthetized by i.p. injection of pentobarbital (50 mg/kg body weight) and immobilized in a Plexiglas tube. The cover glass of the dorsal skinfold chamber was removed and a small piece of the Ultrapro mesh was carefully placed onto the striated muscle tissue within the center of each chamber (Fig. 1b–d), taking care to avoid contamination, mechanical irritation or damage to the chamber preparation.

Intravital fluorescence microscopy

For *in vivo* microscopic observation, the hamsters were again immobilized in a Plexiglas tube and the dorsal skinfold chamber was attached to the microscopic stage. After retrobulbary i.v. injection of 0.1 ml 5% fluorescein isothiocyanate (FITC)-labeled dextran 150 000 (contrast enhancement by staining of blood plasma) and 0.1 ml 0.1% rhodamine 6G (Sigma Aldrich, Taufkirchen, Germany) for direct staining of white blood cells, intravital fluorescence microscopy was performed using a modified Leitz Orthoplan microscope with a 100 W mercury lamp attached to a Ploemo-Pak illuminator with blue, green and ultraviolet filter blocks (Leitz, Wetzlar, Germany) for epi-illumination. The microscopic images were recorded by a charge-coupled device video camera (CF8/1 FMC; Kappa GmbH, Gleichen, Germany) and transferred to a video system for off-line evaluation. With the use of 4×, 6.3×, 10×, and 20× long-distance objectives (Leitz) magnifications of ×86, ×136, ×216 and ×432 were achieved on a 14-inch video screen (PVM 1444; Sony, Tokyo, Japan).

Microcirculatory analysis

The microscopic images were analyzed quantitatively off-line by means of the computer-assisted image analysis system CapImage (Zeintl, Heidelberg, Germany). In four different microvascular regions of interest (ROIs) in the border zone of the meshes, i.e. in close vicinity to the implanted material, we measured leukocyte–endothelial cell interaction within host postcapillary or collecting venules (diameter: approximately 20–40 μm). For this purpose, the leukocytes were classified according to their interaction with the vascular endothelium as adherent, rolling or free-flowing cells [14]. Adherent leukocytes were defined in each vessel segment as cells that did not

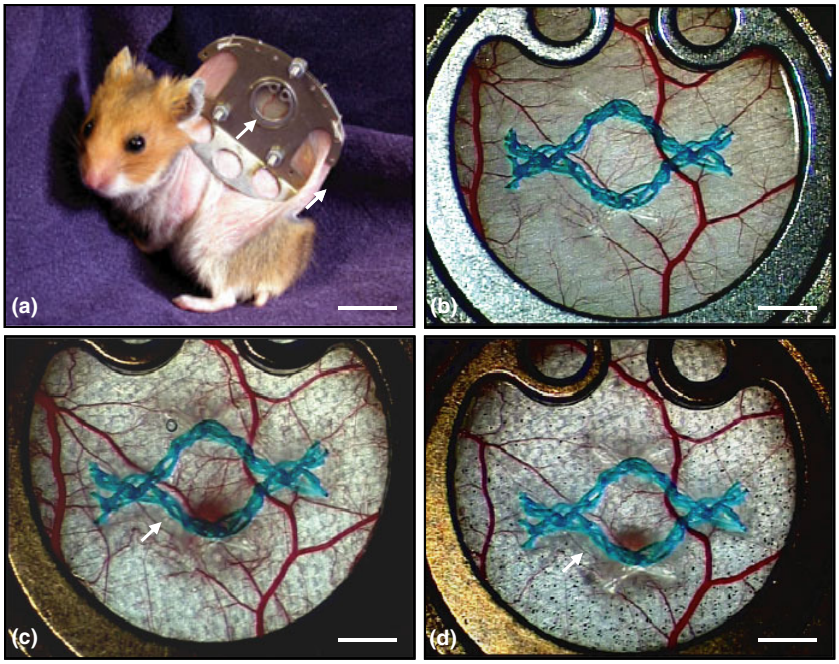

Figure 1 (a) Syrian golden hamster with an implanted dorsal skinfold chamber (chamber weight approximately 4 g). Within the observation window (arrow) arterioles, capillaries and venules of the striated skin muscle and subcutaneous tissue can be analyzed using intravital trans- and epi-illumination microscopy. (b–d) Overview of the observation window after implantation of a small piece of the Ultrapro mesh into the dorsal skinfold chamber of a rapamycin (0.08 mg/kg)-treated animal (b). (c) and (d) display the same implant at days 7 and 14 after implantation. Edema formation (arrow) in direct vicinity to the mesh implant can already be observed macroscopically at day 7 (c) and day 14 (d). However, for a more detailed visualization of blood vessel development at the implantation site high-resolution intravital fluorescence microscopy has to be performed. Scale bars: a = 15 mm; b–d = 1.7 mm.

move or detach from the endothelial lining within an observation period of 20 s, and are given as number of cells per square millimeter of endothelial surface, calculated from the diameter and length of the vessel segment studied, assuming a cylindrical vessel geometry. Rolling leukocytes were defined as cells moving with a velocity less than two-fifths of the centerline velocity, and are given as number of cells per 20 s passing a reference point within the microvessel [15].

Angiogenesis was analyzed in eight different microvascular ROIs in the border zone of the meshes. ROIs were defined as positive for angiogenesis when signs of blood vessel development, i.e. capillary buds and sprouts or newly formed microvessels ingrowing into the surgical mesh implant, could be identified [14]. More detailed information on the vascular ingrowth into the different ROIs was provided by the quantitative analysis of the functional capillary density, i.e. the length of perfused capillaries per observation area given in cm/cm^2 [16].

Experimental protocol

A total of 16 Ultrapro meshes were implanted into dorsal skinfold chambers of Syrian golden hamsters, which were treated daily with 0.08 mg/kg i.p. ($n = 6$) or 1.5 mg/kg i.p. ($n = 5$) rapamycin (Wyeth Pharma GmbH, Münster, Germany) as well as CsA ($n = 5$; 20 mg/kg; Sigma Aldrich). The dosages of rapamycin and CsA used in this study have previously been shown to be effective in various rodent models [17–21]. Immunosuppressive therapy started 48 h before mesh implantation. Additional seven hamsters, which did not receive any immunosuppressant therapy, served as controls. Intravital fluorescence microscopic analysis of leukocyte–endothelial cell interaction and vascularization was performed under baseline conditions (BL) directly before mesh implantation as well as at 20 min, 24 h, 3, 7 and 14 days after mesh implantation. At the end of the *in vivo* experiments, i.e. at day 14, incorporation of the surgical meshes into the surrounding host tissue was analyzed by histologic examinations of the dorsal skinfold chamber preparations. Explantation strength was measured in four additional animals per group. Moreover, blood was drawn from the jugular vein of three additional animals per group in order to measure systemic leukocyte counts and whole blood concentrations of rapamycin and CsA under baseline conditions and after 14 days.

Measurement of explantation strength

Incorporation of the surgical meshes into the surrounding host tissue was controlled by measurement of the explantation strength at day 14 after implantation. For this purpose, animals were anesthetized by i.p. injection of pentobarbital (50 mg/kg body weight), immobilized in a Plexiglas tube and the dorsal skinfold chamber was fixed on a Plexiglas stage. Then, the meshes were fixed at two filaments with 7-0 Prolene sutures connected to a dynamometer and pulling power was increased constantly by 1 cN/mm^2/s [10,22]. The force necessary to tear the meshes out of the surrounding host tissue indicated the explantation strength (cN/mm^2).

Histology

For light microscopy, formalin-fixed specimens of the dorsal skinfold preparations were embedded in paraffin at day 14 after mesh implantation. Four-µm-thick sections were cut and stained with hematoxylin and eosin according to standard procedures. Additional sections were stained with sirius red to detect collagen fibers within the newly formed granulation tissue surrounding the mesh implants.

Statistics

After testing the data for normal distribution and equal variance, differences between the groups were analyzed by ANOVA followed by the appropriate *post hoc* comparison. To test for time effects, ANOVA for repeated measures was applied. This was followed by the paired Student's *t*-test, including correction of the α-error according to Bonferroni probabilities for repeated measurements (SigmaStat; Jandel Corporation, San Rafael, CA, USA). All values are expressed as means ± SEM. Statistical significance was accepted for a *P*-value of <0.05.

Results

Whole blood concentrations of rapamycin and CsA

Whole blood concentrations of rapamycin and CsA were found to be 5 ± 0 µg/l (0.08 mg/kg rapamycin), 120 ± 47 µg/l (1.5 mg/kg rapamycin) and 212 ± 46 µg/l (20 mg/kg CsA) under baseline conditions as well as 3 ± 0 µg/l (0.08 mg/kg rapamycin), 86 ± 33 µg/l (1.5 mg/kg rapamycin) and 342 ± 25 µg/l (20 mg/kg CsA) after 14 days. This indicates that immunosuppressive concentrations were achieved throughout the whole duration of the experiments.

Angiogenesis and vascularization

A first angiogenic response to the surgical meshes could be observed at day 3 after implantation into the dorsal skinfold chamber, as indicated by approximately 40% of angiogenesis positive ROIs in CsA-treated and control hamsters (Fig. 2a). This angiogenic response was characterized by the formation of vessel sprouts originating from the host muscle capillaries and postcapillary venules. During the following days, these sprouts grew into the space between the mesh fibers, and finally interconnected to each other, resulting in the development of new microvascular

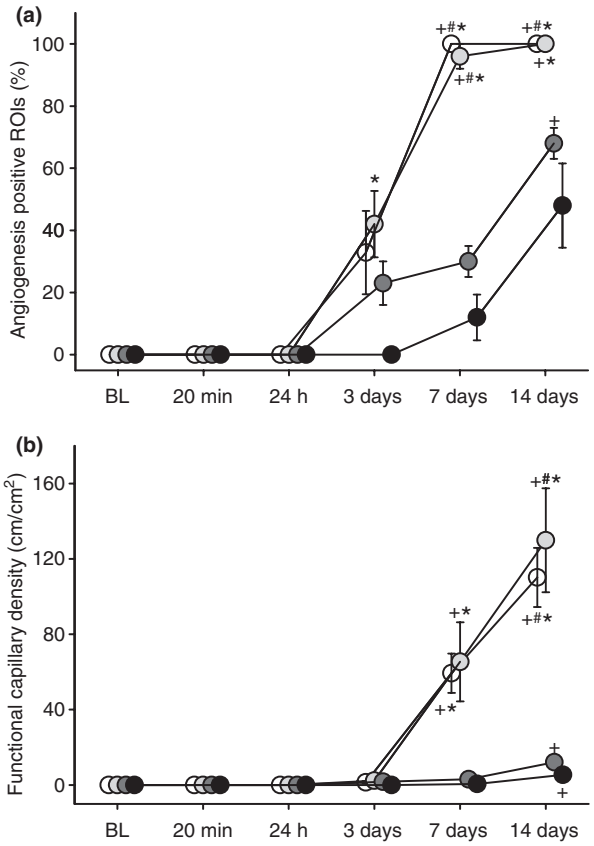

Figure 2 Angiogenesis positive ROIs (%) (a), and functional capillary density of newly formed blood vessels (cm/cm^2) (b) in the border zone of the Ultrapro mesh, as assessed by intravital fluorescence microscopy and computer-assisted image analysis before (BL, baseline) as well as 20 min, 24 h, and 3, 7 and 14 days after implantation into the dorsal skinfold chamber of CsA-treated (light grey circles) and rapamycin (dark grey circles: 0.08 mg/kg; black circles: 1.5 mg/kg)-treated hamsters. Untreated animals (white circles) served as controls. Mean values ± SEM. $^{+}P < 0.05$ versus BL; $^{\#}P < 0.05$ versus rapamycin (0.08 mg/kg)-treated animals at corresponding time points; $^{*}P < 0.05$ versus rapamycin (1.5 mg/kg)-treated animals at corresponding time points.

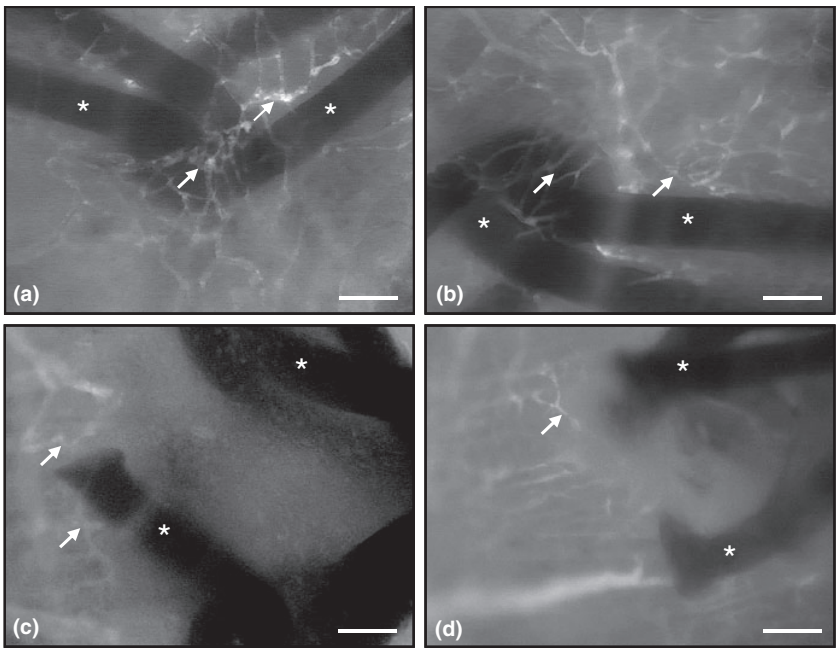

Figure 3 Intravital fluorescence microscopic images of the Ultrapro mesh at day 14 after implantation into the dorsal skinfold chamber of a control hamster (a) and animals treated with CsA (b), 0.08 mg/kg rapamycin (c) or 1.5 mg/kg rapamycin (d). The mesh fibers (asterisks) of the control (a) and the CsA-treated animal (b) are surrounded by a dense network of newly formed microvessels (arrows). In contrast, the granulation tissues around the Ultrapro meshes of the rapamycin-treated animals (c,d) exhibit only a few newly formed blood vessels (arrows). Blue light epi-illumination with contrast enhancement by 5% FITC-labeled dextran 150 000 i.v. Scale bars: 130 μm.

networks surrounding the mesh implants (Fig. 3a and b). At day 14, these networks exhibited a functional capillary density of approximately 110–130 cm/cm^2 without any differences between the CsA and control group (Fig. 2b). In contrast, immunosuppressive therapy with rapamycin dose-dependently inhibited the vascularization process of the mesh implants. Rapamycin (0.08 mg/kg)-treated animals presented with only approximately 20% of angiogenesis-positive ROIs at day 3 after implantation (Fig. 2a), and high-dose (1.5 mg/kg)-treated animals showed even 0% of angiogenesis positive ROIs at the corresponding time point (Fig. 2a). Although the development of new blood vessels could also be observed in this group during the further time course, the angiogenic response to the mesh implants was found to be extremely poor with a final functional capillary density of the newly formed microvascular networks of only approximately 12 cm/cm^2 (0.08 mg/kg rapamycin) and approximately 5 cm/cm^2 (1.5 mg/kg rapamycin) at day 14 (Figs 2b and 3c,d).

Leukocyte–endothelial cell interaction

In control animals, the numbers of rolling and adherent leukocytes were approximately 26 cells/min and 120 cells/

Table 1. Rolling and adherent leukocytes in postcapillary and collecting venules within the border zones of the Ultrapro mesh before (BL, baseline) as well as 20 min, 24 h, and 3, 7 and 14 days after implantation into control, cyclosporine A (CsA)-treated and rapamycin-treated (Rapa; 0.08 or 1.5 mg/kg) animals.

	BL	20 min	24 h	3 days	7 days	14 days
Rolling leukocytes (cells/min)						
Control	25.5 ± 2.7*†	26.1 ± 3.6*	41.8 ± 4.0*†‡	22.6 ± 1.4	23.7 ± 4.0	16.9 ± 3.1
CsA	20.0 ± 1.5†	15.0 ± 1.2	24.5 ± 6.5	27.1 ± 4.2	21.2 ± 4.3	25.2 ± 8.0
Rapa (0.08 mg/kg)	13.5 ± 1.8	16.4 ± 3.8	17.6 ± 4.8	27.2 ± 7.3	34.2 ± 5.0‡	17.4 ± 2.7
Rapa (1.5 mg/kg)	6.6 ± 1.0	10.2 ± 1.7	15.3 ± 1.8	19.1 ± 4.1	17.9 ± 3.0	9.9 ± 4.0
Adherent leukocytes (cells/mm^2):						
Control	118.4 ± 25.6	240.5 ± 98.1	200.5 ± 46.9	112.2 ± 38.3	72.8 ± 14.6	81.2 ± 30.0
CsA	99.5 ± 21.3	224.9 ± 41.4‡	209.0 ± 39.4	98.0 ± 19.5	74.1 ± 24.6	85.0 ± 16.3
Rapa (0.08 mg/kg)	74.9 ± 24.2	211.9 ± 66.4	233.1 ± 45.4‡	58.8 ± 15.3	51.5 ± 23.9	120.8 ± 21.0
Rapa (1.5 mg/kg)	85.8 ± 31.4	69.2 ± 12.9	171.2 ± 42.9	94.4 ± 22.5	76.7 ± 28.0	56.3 ± 24.2

Values are given as mean ± SEM.
*$P < 0.05$ versus rapamycin (0.08 mg/kg)-treated animals at corresponding time points.
†$P < 0.05$ versus rapamycin (1.5 mg/kg)-treated animals at corresponding time points.
‡$P < 0.05$ versus BL.

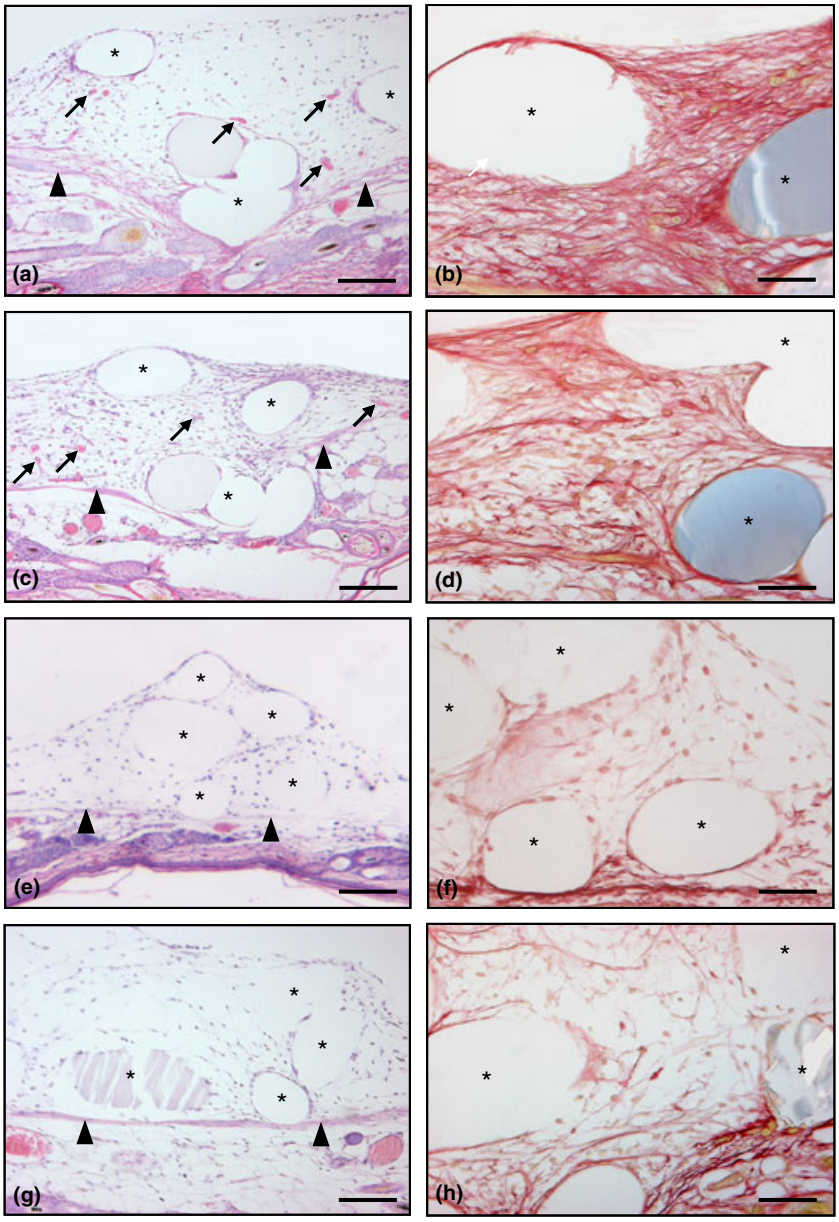

Figure 4 Histologic cross sections of the Ultrapro mesh fibers (indicated by asterisks) at day 14 after implantation onto the striated muscle tissue (arrowheads) within the dorsal skinfold chamber of a control (a,b), a CsA-treated (c,d), a rapamycin (0.08 mg/kg)-treated (e,f) and a rapamycin (1.5 mg/kg)-treated hamster (g,h). Hematoxylin–eosin staining (a,c,e,g) reveals that in contrast to the rapamycin-treated animals (e,g), the meshes of the control (a) and CsA-treated (b) hamster are surrounded by a densely vascularized granulation tissue with many newly formed blood vessels (arrows). As indicated by sirius red staining (b,d,f,h), the granulation tissue in the rapamycin-treated hamsters exhibits a reduced collagen content (f,h) when compared with that of the control (b) and CsA-treated animal (d). Scale bars: a,c,e,g = 200 μm; b,d,f,h = 100 μm.

mm^2 under baseline conditions. Shortly after mesh implantation, leukocyte–endothelial cell interaction was found enhanced, peaking at 24 h with significantly increased numbers of rolling leukocytes. This leukocytic response normalized later on to baseline values and remained constant until the end of the experiments (Table 1). In contrast, CsA- and rapamycin-treated hamsters presented with decreased numbers of rolling leukocytes during the first 24 h of the experiment when compared with controls (Table 1). This effect was most pronounced in the group of rapamycin (1.5 mg/kg)-treated hamsters. Correspondingly, these animals exhibited also a tendency toward a reduced number of adherent leukocytes directly after mesh implantation (Table 1). Between days 3 and 14, however, there were no statistical differences in leukocyte–endothelial cell interaction among the three observation groups (Table 1). Besides, systemic leukocyte counts of rapamycin-treated (0.08 mg/kg: $6.6 \pm 0.6 \times 10^3/\mu l$; 1.5 mg/kg: $8.5 \pm 5.7 \times 10^3/\mu l$), CsA-treated ($13.8 \pm 3.5 \times 10^3/\mu l$) and control animals ($10.9 \pm 2.5 \times 10^3/\mu l$) were comparable under baseline conditions and did not significantly differ from those measured at day 14 (0.08 mg/kg rapamycin: $10.3 \pm 3.1 \times 10^3/\mu l$; 1.5 mg/kg rapamycin: $9.8 \pm 5.4 \times 10^3/\mu l$; CsA: $11.4 \pm 2.8 \times 10^3/\mu l$; control: $9.1 \pm 1.3 \times 10^3/\mu l$), indicating the absence of a systemic inflammatory response.

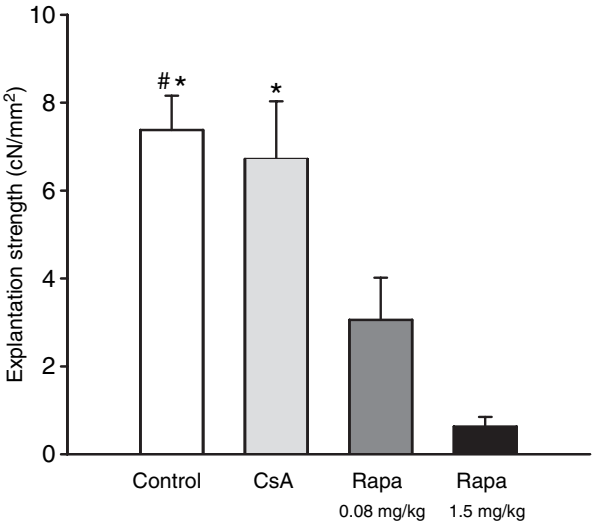

Figure 5 Explantation strength (cN/mm^2) at day 14 after implantation of the Ultrapro mesh into the dorsal skinfold chambers of CsA-treated and rapamycin (Rapa; 0.08 or 1.5 mg/kg)-treated hamsters. Untreated animals served as controls. For the measurement, the mesh was fixed at two filaments with 7-0 Prolene sutures connected to a dynamometer and pulling power was increased constantly by 1 cN/mm^2/s. The force necessary to tear the mesh out of the surrounding host tissue indicated the explantation strength. Mean values ± SEM. $^{\#}P < 0.05$ versus rapamycin (0.08 mg/kg)-treated animals; $^{*}P < 0.05$ versus rapamycin (1.5 mg/kg)-treated animals.

Mesh incorporation

Histologic examinations of the dorsal skinfold chamber preparations at day 14 after mesh implantation demonstrated that the Ultrapro meshes were surrounded by a newly formed granulation tissue in all three experimental groups (Fig. 4a,c,e and g). However, corresponding to our intravital microscopic findings, the granulation tissue in both low-dose and high-dose rapamycin-treated animals exhibited only a few newly developed blood vessels when compared with the well-vascularized granulation tissue of the other two groups (Fig. 4a,c,e and g). Moreover, sirius red staining revealed that the immunosuppressant therapy with low-dose and high-dose rapamycin markedly reduced the amount of collagen fibers in the granulation tissue (Fig. 4b,d,f and h).

In line with our histologic findings, the measurement of the explantation strength demonstrated a dose-dependently impaired incorporation of the Ultrapro meshes of rapamycin-treated animals into the surrounding host tissue with an over 50% and 90% reduced explantation strength of approximately 3.1 cN/mm^2 (0.08 mg/kg rapamycin) and approximately 0.6 cN/mm^2 (1.5 mg/kg rapamycin) when compared with that of CsA-treated animals and controls (approximately 7 cN/mm^2) (Fig. 5).

Discussion

In this *in vivo* study, we could demonstrate that in contrast to immunosuppressive therapy with CsA, administration of rapamycin dose-dependently impairs vascularization and incorporation of implanted surgical meshes. This result is of major clinical importance considering the fact that the incidence of incisional hernias following orthotopic liver transplantation has been reported to be increasing during the last few years [1]. Our results indicate now that transplant patients should not be treated with rapamycin during the initial phase after incisional hernia repair in order to guarantee adequate mesh incorporation and, thus, to reduce the risk of recurrence.

Since 1999, rapamycin has been approved by the United States Food and Drug Administration as an immunosuppressive drug for the prophylaxis of organ rejection [23]. In contrast to the calcineurin inhibitors CsA and tacrolimus, which interfere with interleukin-2 gene transcription [24,25], rapamycin forms a complex with the immunophilin FK506 binding protein-12, resulting in the inhibition of the regulatory kinase mammalian target of rapamycin [23]. This leads to the arrest of the cell-cycle at the G1 to S phase. Hence, T-lymphocyte activation and proliferation as well as antibody production is suppressed [23]. Thus, rapamycin in combination with other immunosuppressants, such as corticosteroids, may offer the possibility of withdrawing or avoiding nephrotoxic calcineurin-inhibitors in kidney transplantation [26]. Importantly, besides its effects on the immune system, rapamycin has also been shown to inhibit tumor growth [17,27], which makes it attractive for patients undergoing liver transplantation for hepatocellular carcinoma [2].

However, rapamycin also bears some important disadvantages. Several studies reported that rapamycin causes higher rates of wound complications when compared with other immunosuppressive drugs [28,29]. This is because of the fact that rapamycin inhibits angiogenesis by down-regulation of vascular endothelial growth factor (VEGF) expression [6]. Accordingly, we could demonstrate in this study that vascularization of implanted meshes in hamsters treated with low and high doses of rapamycin was markedly reduced when compared with CsA-treated and control animals.

Angiogenesis is a major prerequisite for the rapid formation of a stable granulation tissue. For instance, Dubay *et al.* [30] reported in an experimental study that angiogenesis could markedly be accelerated and improved in abdominal fascial incisions of rats during the first four postoperative weeks by implanting a sustained-release polymer of basic fibroblast growth factor. Interestingly, this resulted in a significantly reduced formation of incisional hernias attributable to an increased stability of the wounds.

Relating to our study, this means that the early angiogenic response to a surgical mesh could be a critical determinant for adequate mesh incorporation. Thus, mesh vascularization might be an indicator for the prediction of the long-term outcome of mesh-stabilized abdominal wall defects.

Because it is well known that inflammation is a major stimulus for angiogenesis [31], we also analyzed leukocyte–endothelial cell interaction in venules located in direct vicinity to the mesh implants. As reported previously [10], we could demonstrate that mesh implantation resulted in a short-term increase of leukocyte–endothelial cell interaction in control animals. Interestingly, this could not be observed in animals treated with high doses of rapamycin, which might be attributable to the fact that rapamycin has been shown to reduce the expression of adhesion molecules such as vascular cell adhesion molecule (VECAM) and P-selectin [32]. However, it is unlikely that this was the cause for the observed differences in the vascularization process of the surgical meshes under analysis, because after 3 days, there were no more differences in numbers of rolling and adherent leukocytes among the experimental groups. Moreover, we also showed a slight reduction in leukocyte rolling in the CsA-treated group when compared with controls, although both groups exhibited an identical angiogenic host tissue response to the mesh implants. Finally, hamsters treated with only 0.08 mg/kg rapamycin presented with numbers of adherent leukocytes, which were comparable to those of the control and CsA group, whereas blood vessel ingrowth into the mesh implants was significantly inhibited by this low-dose treatment. Therefore, we suggest that the observed anti-angiogenic effect of rapamycin is most probably caused by the specific inhibition of angiogenic growth factors, such as VEGF, and not by the generalized suppression of inflammatory processes.

Our histologic analyses revealed that besides the inhibition of angiogenesis, administration of rapamycin resulted in the reduction of collagen deposition within the granulation tissue surrounding the implanted meshes. Accordingly, mesh incorporation was massively impaired, as indicated by a significantly decreased explantation strength at day 14 after implantation when compared with CsA-treated and control animals. These findings are in line with earlier studies, reporting a direct inhibitory effect of rapamycin on the expression of important extracellular matrix proteins, including fibronectin, α-smooth muscle actin and collagen [33,34]. For this reason, rapamycin has also been suggested as a potential therapeutic target for the treatment of keloids and excessive scars and coronary re-stenosis [34,35]. On the other hand, rapamycin might have indirectly suppressed collagen synthesis in this study by inhibition of nitric oxide (NO). In fact, the granulation tissue around implanted meshes contains many macrophages and fibroblasts. These cell types have been shown to produce NO during wound healing, resulting in an increased collagen formation and mechanical strength of wounds [36,37]. However, Schäffer *et al.* [6] recently demonstrated that this mechanism is inhibited by application of rapamycin. We suggest now that the effects of rapamycin on extracellular matrix formation do not only play an important role in wound healing, but also in cases of biomaterial incorporation and engraftment.

In summary, we could show in the present *in vivo* study that immunosuppressive therapy with rapamycin impairs incorporation of surgical meshes by inhibition of angiogenesis and collagen synthesis within the newly developing granulation tissue around the implants. Therefore, we postulate that immunosuppressed patients should not be treated with rapamycin in case of incisional hernia repair by mesh implantation.

Authorship

MWL: designed the study and wrote the paper. JMH and JR: performed the study and analyzed data. HS: performed whole blood analysis. MDM: designed the study and revised the paper.

Funding

This work was supported by the research program of the Medical Faculty of the University of Saarland (HOMFOR 06/79).

Acknowledgements

We are grateful to Janine Becker for the excellent technical assistance.

References

1. Kahn J, Müller H, Iberer F, *et al.* Incisional hernia following liver transplantation: incidence and predisposing factors. *Clin Transplant* 2007; **21**: 423.
2. Toso C, Meeberg GA, Bigam DL, *et al.* De novo sirolimus-based immunosuppression after liver transplantation for hepatocellular carcinoma: long-term outcomes and side effects. *Transplantation* 2007; **83**: 1162.
3. Piazzese E, Montalti R, Beltempo P, *et al.* Incidence, predisposing factors, and results of surgical treatment of incisional hernia after orthotopic liver transplantation. *Transplant Proc* 2004; **36**: 3097.
4. Kelley SF, Felix AM, Ehrlich HP. The antagonism of glucocorticoid inhibition of wound healing in rats by growth hormone-releasing factor. *Proc Soc Exp Biol Med* 1990; **194**: 320.

5. Guilbeau JM. Delayed wound healing with sirolimus after liver transplant. *Ann Pharmacother* 2002; **36**: 1391.
6. Schäffer M, Schier R, Napirei M, Michalski S, Traska T, Viebahn R. Sirolimus impairs wound healing. *Langenbecks Arch Surg* 2007; **392**: 297.
7. Mekeel K, Mulligan D, Reddy KS, Moss A, Harold K. Laparoscopic incisional hernia repair after liver transplantation. *Liver Transpl* 2007; **13**: 1576.
8. Luijendijk RW, Hop WC, van den Tol MP, *et al.* A comparison of suture repair with mesh repair for incisional hernia. *N Engl J Med* 2000; **343**: 392.
9. Zanghì A, Di Vita M, Lomenzo E, De Luca A, Cappellani A. Laparoscopic repair vs open surgery for incisional hernias: a comparison study. *Ann Ital Chir* 2000; **71**: 663.
10. Laschke MW, Häufel JM, Thorlacius H, Menger MD. New experimental approach to study host tissue response to surgical mesh materials in vivo. *J Biomed Mater Res A* 2005; **74**: 696.
11. Roller J, Laschke MW, Sethi S, Herrmann M, Menger MD. Prolene-Monocryl-composite meshes do not increase microvascular Staphylococcus aureus adherence and do not sensitize for leukocytic inflammation. *Langenbecks Arch Surg* 2008; **393**: 349.
12. Endrich B, Asaishi K, Götz A, Messmer K. Technical report – a new chamber technique for microvascular studies in unanesthetized hamsters. *Res Exp Med (Berl)* 1980; **177**: 125.
13. Menger MD, Laschke MW, Vollmar B. Viewing the microcirculation through the window: some twenty years experience with the hamster dorsal skinfold chamber. *Eur Surg Res* 2002; **34**: 83.
14. Laschke MW, Witt K, Pohlemann T, Menger MD. Injectable nanocrystalline hydroxyapatite paste for bone substitution: in vivo analysis of biocompatibility and vascularization. *J Biomed Mater Res B Appl Biomater* 2007; **82**: 494.
15. Menger MD, Pelikan S, Steiner D, Messmer K. Microvascular ischemia-reperfusion injury in striated muscle: significance of ''reflow paradox''. *Am J Physiol* 1992; **263**: H1901.
16. Rücker M, Laschke MW, Junker D, *et al.* Angiogenic and inflammatory response to biodegradable scaffolds in dorsal skinfold chambers of mice. *Biomaterials* 2006; **27**: 5027.
17. Guba M, von Breitenbuch P, Steinbauer M, *et al.* Rapamycin inhibits primary and metastatic tumor growth by antiangiogenesis: involvement of vascular endothelial growth factor. *Nat Med* 2002; **8**: 128.
18. Vajkoczy P, Vollmar B, Wolf B, Menger MD. Effects of cyclosporine A on the process of vascularization of freely transplanted islets of Langerhans. *J Mol Med* 1999; **77**: 111.
19. Laschke MW, Elitzsch A, Scheuer C, Holstein JH, Vollmar B, Menger MD. Rapamycin induces regression of endometriotic lesions by inhibiting neovascularization and cell proliferation. *Br J Pharmacol* 2006; **149**: 137.
20. Holstein JH, Klein M, Garcia P, *et al.* Rapamycin affects early fracture healing in mice. *Br J Pharmacol* 2008; **154**: 1055.
21. Stepkowski SM. Preclinical results of sirolimus treatment in transplant models. *Transplant Proc* 2003; **35**: 219S.
22. Menger MD, Walter P, Hammersen F, Messmer K. Quantitative analysis of neovascularization of different PTFE-implants. *Eur J Cardiothorac Surg* 1990; **4**: 191.
23. Paghdal KV, Schwartz RA. Sirolimus (rapamycin): from the soil of Easter Island to a bright future. *J Am Acad Dermatol* 2007; **57**: 1046.
24. Quesniaux VF. Immunosuppressants: tools to investigate the physiological role of cytokines. *BioEssays* 1993; **15**: 731.
25. Kang HG, Zhang D, Degauque N, Mariat C, Alexopoulos S, Zheng XX. Effects of cyclosporine on transplant tolerance: the role of IL-2. *Am J Transplant* 2007; **7**: 1907.
26. Guerra G, Srinivas TR, Meier-Kriesche HU. Calcineurin inhibitor-free immunosuppression in kidney transplantation. *Transpl Int* 2007; **20**: 813.
27. Guba M, Koehl GE, Neppl E, *et al.* Dosing of rapamycin is critical to achieve an optimal antiangiogenic effect against cancer. *Transpl Int* 2005; **18**: 89.
28. Dean PG, Lund WJ, Larson TS, *et al.* Wound-healing complications after kidney transplantation: a prospective, randomized comparison of sirolimus and tacrolimus. *Transplantation* 2004; **77**: 1555.
29. Kuppahally S, Al-Khaldi A, Weisshaar D, *et al.* Wound healing complications with de novo sirolimus versus mycophenolate mofetil-based regimen in cardiac transplant recipients. *Am J Transplant* 2006; **6**: 986.
30. Dubay DA, Wang X, Kuhn MA, Robson MC, Franz MG. The prevention of incisional hernia formation using a delayed-release polymer of basic fibroblast growth factor. *Ann Surg* 2004; **240**: 179.
31. Costa C, Incio J, Soares R. Angiogenesis and chronic inflammation: cause or consequence? *Angiogenesis* 2007; **10**: 149.
32. Wood SC, Bushar G, Tesfamariam B. Inhibition of mammalian target of rapamycin modulates expression of adhesion molecules in endothelial cells. *Toxicol Lett* 2006; **165**: 242.
33. Shegogue D, Trojanowska M. Mammalian target of rapamycin positively regulates collagen type I production via a phosphatidylinositol 3-kinase-independent pathway. *J Biol Chem* 2004; **279**: 23166.
34. Ong CT, Khoo YT, Mukhopadhyay A, *et al.* mTOR as a potential therapeutic target for treatment of keloids and excessive scars. *Exp Dermatol* 2007; **16**: 394.
35. Abizaid A. Sirolimus-eluting coronary stents: a review. *Vasc Health Risk Manag* 2007; **3**: 191.
36. Schäffer MR, Tantry U, van Wesep RA, Barbul A. Nitric oxide metabolism in wounds. *J Surg Res* 1997; **71**: 25.
37. Yamasaki K, Edington HD, McClosky C, *et al.* Reversal of impaired wound repair in iNOS-deficient mice by topical adenoviral-mediated iNOS gene transfer. *J Clin Invest* 1998; **101**: 967.